



Trade Science Inc.

ISSN : 0974 - 7486

Volume 8 Issue 12

Materials Science

An Indian Journal

Full Paper

MSAIJ, 8(12), 2012 [482-487]

Effect of post synthesis hydrothermal treatment on thioglycolic acid-capped CdSe quantum dots

Rasha G.Ahmed^{1,2*}, Nasser Y.Mostafa^{1,2}

¹Chemistry Department, Faculty of Science, Taif University, Taif- 888, (KINGDOM OF SAUDI ARABIA)

²Chemistry Department, Faculty of Science, Suez Canal University, Ismailia 41522, (EGYPT)

E-mail: nmost69@gmail.com

Received: 11th May, 2012 ; Accepted: 29th September, 2012

ABSTRACT

CdSe quantum dots (QDs) were prepared by using a simple green route with CdSO₄ and Na₂SeSO₃ in aqueous solution. Post synthesis hydrothermal modification of CdSe QDs was performed to enhance the optical properties. The as prepared and the hydrothermally treated thioglycolic acid-capped CdSe quantum dots were characterized by Ultraviolet–visible (UV–vis) spectroscopy, X-ray diffraction (XRD), transmission electron microscopy (TEM) and photoluminescence (PL) spectroscopy. Results demonstrated that CdSe QDs synthesized in aqueous solution showed a zinc-blende structure and a homogeneous size distribution with a mean particle size of about ranging from 2.1 to 2.7 nm. The hydrothermal treatment slightly increases the QDs sizes and enhance the quantum yield (QY).

© 2012 Trade Science Inc. - INDIA

KEYWORDS

CdSe;
Quantum dots;
Hydrothermal;
Green synthesis.

INTRODUCTION

Colloidal semiconductor nanocrystals, often referred to as “quantum dots” (QDs), have gained increasing attention through their unique optical properties^[1-6]. CdSe QDs have been broadly investigated for different applications, like cellular imaging^[7-9], bio-probes,^[10-12] and solar cells^[13,14]. Generally, two main routes have been used for the synthesis of CdSe QDs; organometallic route^[15-17] and aqueous routes^[18,19]. Organometallic route is the most conventional because it produces QDs with good properties, such as high photoluminescence (PL) quantum yield and excellent monodispersity. But, the produced hydrophobic ligands capped QDs cannot be directly used in biological sys-

tem. However, the aqueous synthesis route, producing QDs with several advantages such as excellent water solubility and biological compatibility^[10]. The disadvantage of the aqueous route is the low quantum yield compared to the organic method. Until now, the design of water-soluble QDs with high quantum yield is still one of the research areas^[21-25]. Recently, Xue et al.^[26] reported highly luminescent water-soluble CdSe QDs, which were first prepared using thioglycolic acid (TGA) as a ligand and were then covalently coupled with target bacteria. Shang and Wang^[27] demonstrated triethanolamine-capped CdSe QDs as fluorescent sensors for reciprocal recognition of Hg²⁺ and iodide in aqueous solution. Su et al.^[28] reported that mercaptosuccinic acid (MSA) capped CdSe QDs were prepared at the po-

larizable interface between water and 1,2-dichloroethane electrolyte solutions by electrochemical method.

In this paper, we report the effect of post synthesis hydrothermal treatments of CdSe QDs on the particle sizes and quantum yield.

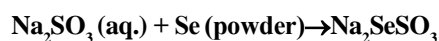
MATERIALS AND METHODS

Materials

Analytical grade reagents of cadmium sulfate (CdSO_4 , 99+%), selenium powder (Se, 99+%), sodium sulfite (Na_2SO_3), sodium hydroxide (NaOH) and thioglycolic acid (HSCH_2COOH , TGA) (99%) were used as received. Rhodamine 6G (with a photoluminescence quantum yield of 95% in anhydrous ethanol)

Preparation of water soluble CdSe nanoparticles

Sodium selenosulfate (Na_2SeSO_3) solutions were prepared dissolving elemental selenium powder (0.098 g), Na_2SO_3 (0.5 g) and Milli-Q water (20 mL) were mixed thoroughly in three-necked round bottom flask and refluxed for 3.5 h with magnetic stirring. The disappearance of the black coloured Se and the formation of a clear solution suggested the complete conversion of Se into Na_2SeSO_3 , according to the following equation:



The temperature of the mixture was brought down to ambient temperature and the mixture was filtered through Whatmann filter paper. The filtrate obtained was diluted to 25 mL in standard measuring flask with Milli-Q water to prepare 50 mM, Na_2SeSO_3 solution. This freshly prepared solution was used directly for CdSe QD synthesis. For the preparation of CdSe QD with different particle sizes, we used^[29].

A typical synthetic procedure of the CdSe QDs is briefly described below. First, certain volume of 0.2 M CdSO_4 solution and 0.6 ml of TGA were added to 200 ml of double distilled with rapid stirring. The pH was adjusted to 8 unites using 1 M NaOH solution. Then 6 mL of sodium selenosulfate solution (0.4 M) (containing about 2.4 mmol of Se precursor) was swiftly injected into solution with rapid stirring. To prepare CdSe QDs with different particle size the $[\text{Cd}^{2+}]/[\text{Se}^{2-}]$ ratios was varied as 2.0, 1.6, 1.2, 1.0 and 0.8. The tempera-

ture was maintained at room temperature for the growth of CdSe QDs according to the following equation:

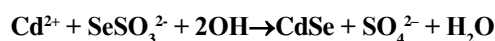


TABLE 1 : Cd/Se molar ratios for different preparation of CdSe QDs

| Sample | Cd/Se ratio | Se (ml) | Cd (ml) | Se (mole) |
|--------|-------------|---------|---------|-----------|
| CdSe1 | 2 | 6 | 24 | 2.4 |
| CdSe2 | 1.6 | 6 | 19.2 | 2.4 |
| CdSe3 | 1.2 | 6 | 14.4 | 2.4 |
| CdSe4 | 1.0 | 6 | 12 | 2.4 |
| CdSe5 | 0.8 | 6 | 9.6 | 2.4 |

Finally methanol was added to precipitate CdSe QDs. The precipitated CdSe QDs were separated by centrifugation, further washed with methanol several times, and dried in the air at 50 °C for characterization. Microwave hydrothermal treatments of CdSe QDs suspended in water were carried out in microwave digestion system (CEM Corporation, Matthew, NC, USA) at 120°C for 10 mintues.

Characterization methods

X-ray diffraction (XRD) analysis was performed using an automated diffractometer (Philips type: PW1840), at a step size of 0.02°, scanning rate of 2° in 2θ/min., and a 2θ range from 4° to 80°. The shape and particle size distribution were studied using transmission electron microscope operated at 120 kV accelerating voltage (JTEM-1230, Japan, JEOL). The samples were prepared by making a suspension from the powder in distilled water using ultrasonic water bath. Then a drop of the suspension was put into the carbon grid and left to dry. The Attenuated Total Reflectance-Fourier Transform Infrared spectra of QDs have been obtained by a ALPHA FT-IR Spectrometer, BRUCKER.

The optical properties of CdSe nanocrystals were studied through optical absorption and photoluminescence measurements. Room temperature UV-vis absorption spectra were measured by Perkin Elmer spectrophotometer along the wavelength range 200–8000 nm. The photoluminescence was measured at room temperature using Perkin Elmer LS 55 Fluorescence Spectrometer with the excitation wavelength of 365 nm. These optical measurements were carried out by preparing a suspension solution of CdSe quantum dots in

Full Paper

chloroform. This suspension put into quartz cuvette for optical absorption and photoluminescence measurements.

The diameters of CdSe QDs were calculated from the excitonic absorption peak using a simple effective mass approximation (EMA) model proposed by Brus^[30]. In the strong-confinement regime, the confinement energy of the first excited electronic state can be approximated by the Brus equation:

$$E_R = E_g^{\text{bulk}} + \frac{h^2}{8r^2} \left[\frac{1}{m_0 m_e^*} + \frac{1}{m_0 m_h^*} \right] - \frac{1.8e^2}{8\pi \Sigma \Sigma_0 r}$$

where E_R is the band gap energy, which is calculated from the transmittance spectrum, E_g^{bulk} is the bulk band gap, h is Planck's constant, r is the particle radius, m_e^* and m_h^* are the effective mass of electrons and holes, respectively; m_0 and e are the mass and charge of a free electron, respectively; Σ_0 is the permittivity of free space, and Σ is the relative permittivity. The band gap (E_R) of QDs can be determined from the absorbance. In this case, the particle size of QDs can be calculated by taking $E_g^{\text{bulk}} = 1.42\text{eV}$, $\Sigma = 6.1$, $m_e^* = 0.13$ and $m_h^* = 0.6$ ^[31] and^[32]. Thus, the particle diameters of CdSe QDs are calculated at different Cd/Se ratios.

The photoluminescence quantum yield (QY) was obtained by comparison with a standard (Rhodamine 6G in ethanol) and using data derived from the luminescence and the absorption spectra^[33], according to Demas and Crosby method^[34]. Here, Rhodamine 6G (R6G) dye, (QY(R6G) = 95% in ethanol), is used as reference, and excitation is kept at 480 nm.

$$QY(\text{CdSe}) = QY(\text{R6G}) \cdot \frac{FR6G}{FOD} \cdot \frac{ODR6G}{ODQD} \cdot \left(\frac{RQD}{RR6G} \right)^2$$

where, FQD and FR6G are the integrated fluorescence emission intensities, ODR6G and ODQD are the optical densities of the samples at 480 nm, RQD and RR6G are the refractive indices for the solvents.

RESULTS AND DISCUSSION

XRD patterns

The CdSe QDs were synthesized over a wide of Cd/Se ratios from 2 to 0.8 in aqueous solution. The as-

synthesized QDs were isolated from solutions using ethanol and centrifugation. The powders were then characterized by XRD method and the results are shown in Figure 1. Figure 1, shows XRD pattern of CdSe QDs prepared at Cd/Se ratio of 1.2 (CdSe3). The broadening of the diffraction peaks indicated the small size of the obtained CdSe QDs. These diffraction features appearing at 27.3°, 45.8°, and 49.2° correspond to the (1 1 1), (2 2 0), and (3 1 1) planes of zinc-blende structure (cubic), respectively with the cell constant $a = 6.07 \text{ \AA}$ (JCPDS No. 03-065-2891). The humps at 45.8° were supposed to be a result of the integration of the peak (220) and peak (311).

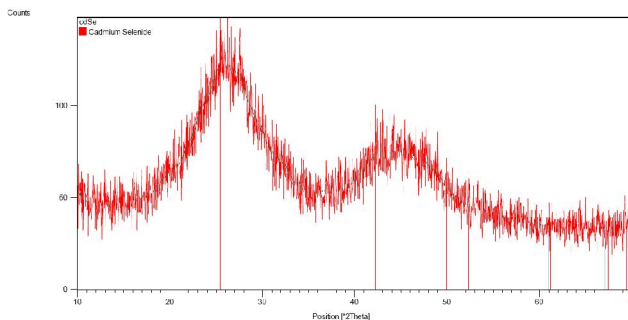


Figure 1 : X-ray diffraction pattern of CdSe QDs prepared at Cd/Se ratio of 1.2 (CdSe3)

TEM observation

TEM images of CdSe QDs were used to determine the size and the shape of CdSe QDs. The as-prepared CdSe QDs sample made with Cd/Se ratio of 2.2 (CdSe3) is shown in Figure 2. As seen, the QDs synthesized in this study consisted of basically round particles. Most of these particles were of 2 ~ 3 nm. The selected area electron diffraction (SAED) patterns of the QDs were also shown in Figure 3. Three concentric rings were observed, giving interplanar distances of 0.332, 0.203 nm and 0.171 nm. Note that there had three diffraction peaks at 27.3°, 45.8°, and 49.2° for the CdSe QDs and the corresponded interplanar distances were 0.351, 0.215, and 0.183 nm. Thus the TEM and SAED results of the QDs were in good agreement with those of the XRD pattern. Another interesting point was that the two concentric rings in Figure 3 were visibly broadened, a sign of interplanar distanced distribution of the QDs. Thus, the rather flat humps in Figure 1 was related probably not only to the particle refinement but also to the interplanar distance distribution of the QDs.

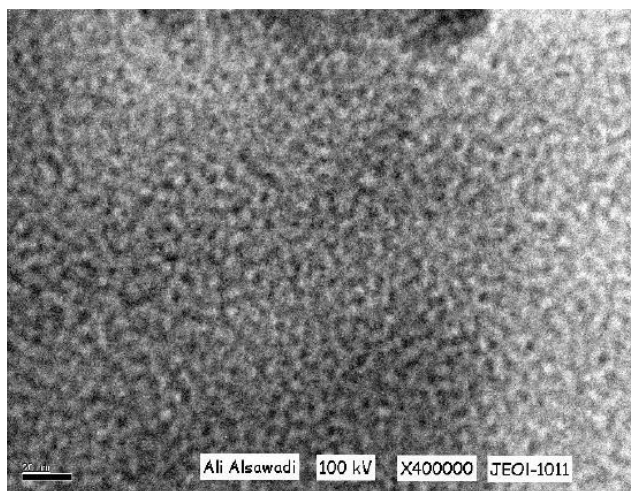


Figure 2 : TEM images of CdSe QDs prepared with Cd/Se ratio of 1.2 (sample CdSe3)

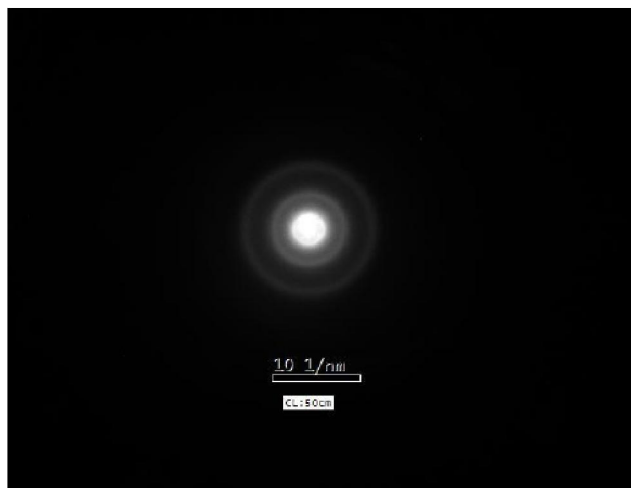


Figure 3 : Selected area electron diffraction (SAED) of CdSe QDs (sample CdSe3)

FTIR spectra

The FTIR spectra of TGA-capped CdSe QDs are shown in Figure 2b. The spectra clearly shows the interaction between TGA and CdSe QDs. As shown in Figure 2, a broad absorption band around 3400 cm^{-1} is assigned to O–H vibration of the absorbed H_2O . The stretching vibration of the thiol group (2550 cm^{-1}) was absent. As reported^[35], due to the formation of covalent bonds between thiols and the Cd^{2+} ions of the surface of QDs, the peaks of –SH group on the surface of QDs disappeared. It disclosed that TGA-capped CdSe QDs were formed. The characteristic absorption band of C=O vibration shifts from 1700 cm^{-1} to 1626 cm^{-1} . Therefore, these results strongly suggest that the thiol groups of TGA coordinate with Cd^{2+} ions on the QDs

surface, and the hydrophilic hydroxyl groups face outward, making QDs water-soluble.

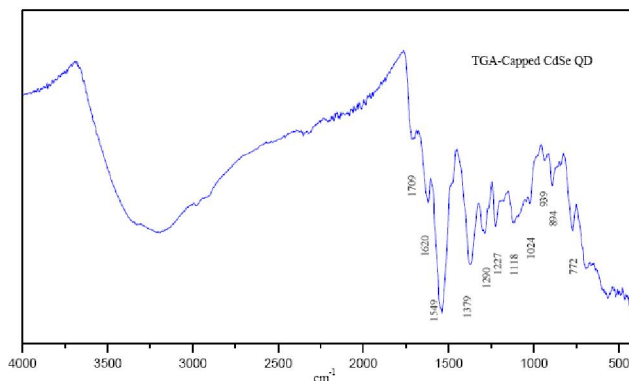


Figure 4 : FT-IR spectra of CdSe QDs capped with TGA

UV spectra

Typical UV–vis absorption spectra of the obtained CdSe QDs with different sizes are presented in Figure 5. The UV–vis absorption edge of CdSe QDs showed an obvious red-shift with decreasing the Cd/Se molar ratio, indicating the effect of quantum confinement. From quantum size effects, the redshifts of the absorption peak indicated the increase of particle size. Hence the size-tuning of CdSe QDs was easily achieved by controlling the molar Cd/Se ratios in reaction media. The excitonic absorption peak was not very distinct, indicating the formation of CdSe QDs with wide particle size distribution. The diameters of CdSe QDs before and after microwave hydrothermal treatment were calculated from the excitonic absorption peak using a simple effective mass approximation (EMA) model proposed by Brus^[30].

The results revealed that the particle diameter and the concentration of the as-prepared CdSe QDs were approximately in the range 2.1 to 1.7 nm. As can be seen, the CdSe QDs exhibited very broad bands attributed to defect-related emission^[36]. The reason for the generation of defect-related emission may be that the extremely small diameter has a very high surface-to-volume ratio, and the high-density dangling bonds and trap sites on the surface are easy to be formed and difficult to be passivated.

Figure 6, shows the UV absorption spectra of CdSe QDs after microwave hydrothermal treatment at 110°C for 10 minutes. The microwave hydrothermal treatment of QDs at results in a systematic red-shift in all samples. As shift in wave length (nm) and particle sizes of QDs

Full Paper

before and after microwave hydrothermal treatment at 110°C are summarized in TABLE 2.

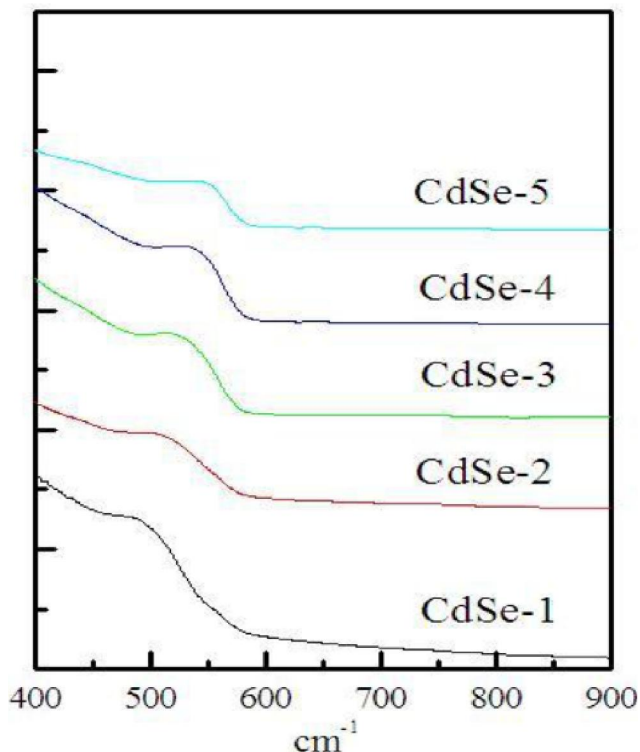


Figure 5 : UV absorption spectra of CdSe QDs before microwave hydrothermal treatment

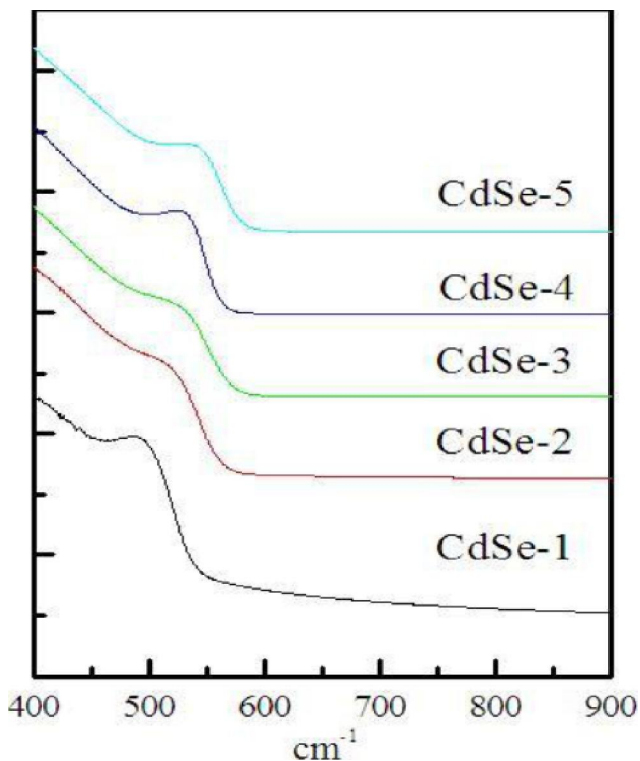


Figure 6 : UV absorption spectra of CdSe QDs after microwave hydrothermal treatment at 110°C for 10 minutes

TABLE 2 : UV adsorption wave length (nm) and particle sizes of QDs prepared with TGA as capping agent, before and after hydrothermal treatment at 110°C

| sample | Before treatment | | After treatment | |
|--------|------------------|---------------|-----------------|---------------|
| | λ (nm) | Diameter (nm) | λ (nm) | Diameter (nm) |
| CdSe 1 | 476 | 2.14 | 487 | 2.23 |
| CdSe 2 | 500 | 2.35 | 524 | 2.61 |
| CdSe 3 | 525 | 2.63 | 531 | 2.71 |
| CdSe 4 | 529 | 2.67 | 535 | 2.77 |
| CdSe 5 | 533 | 2.74 | 539 | 2.84 |

Quantum yield (QY)

The quantum yield (QY) was obtained by using a conventional route, integrating the PL band of CdSe in chloroform and comparing the intensity to that of Rhodamine 6G in anhydrous ethanol. TABLE 3, gives the quantum Yield (QY) of CdSe QDs prepared with TGA as capping agent, before and after hydrothermal treatment at 110°C. The photoluminescence quantum efficiency of as-prepared CdSe QDs at room temperature shows low quantum yield values between 5.4-1.5. Generally, the quantum yield decreases as the QD size increases. Microwave hydrothermal treatment of QDs at 110°C for 10 minutes increases the QY. This enhancement of the QY may be attributed the better passivation of surface traps participating in the non-radioactive recombination processes^[37]. This results from the hydrothermal treatments.

TABLE 3 : Quantum yield (QY) of CdSe QDs prepared with TGA as capping agent, before and after microwave hydrothermal treatment at 110°C

| Sample | QY (%) | |
|--------|--------|-------|
| | Before | After |
| CdSe1 | 5.4 | 7.2 |
| CdSe2 | 4.3 | 5.1 |
| CdSe3 | 3.1 | 4.4 |
| CdSe4 | 2.3 | 3.1 |
| CdSe5 | 1.5 | 2.5 |

CONCLUSIONS

In summary, TGA-capped CdSe QDs were successfully synthesized in aqueous medium. The synthesis of CdSe QDs is facile and can be easily scaled for large amount synthesis. The crystal structure of CdSe

QDs have zinc-blende structure as confirmed by X-ray powder diffraction as well as Selected Area Electron diffraction (SAED) (along with TEM). The size of the prepared QDs can be controlled by the Cd/Se molar ratio in the reaction media. The quantum yield (QY) and the mean size increased by microwave hydrothermal treatments at 110°C for 10 min.

ACKNOWLEDGEMENTS

This work was supported by Taif University, KSA, Project (1365-432-1).

REFERENCES

- [1] N.Herron, Y.Wang, H.Echert; *J.Am.Chem.Soc.*, **109**, 5049 (1987).
- [2] M.C.Schlamp, X.G.Peng, A.P.Alivisatos; *J.Appl. Phys.*, **82**, 5837 (1997).
- [3] T.Trindale, P.O'Brien, N.L.Pickett; *Chem.Mater.*, **13**, 3843 (2001).
- [4] P.J.Costanzo, T.E.Patten, T.A.P.Seery; *Chem. Mater.*, **16**, 1775 (2004).
- [5] J.L.West, N.Halas; *Annu.Rev.Biomed. Eng.*, **5**, 285 (2003).
- [6] H.R.Zhang, C.M.Shen, S.T.Chen, Z.C.Xu, F.S.Liu, J.Q.Li, H.J.Gao; *Nanotechnology*, **16**, 267 (2005).
- [7] P.J.Costanzo, E.Liang, T.E.Patten, S.D.Collins, R.L.Smith; *Lab.Chip.*, **5**, 606 (2005).
- [8] X.Duan, Y.Huang, R.Agarwal, C.M.Lieber; *Nature*, **421**, 241 (2003).
- [9] Y.Jing, W.J.Zhang, J.S.Jie, X.M.Meng, J.A.Zapfen, S.T.Lee; *Adv.Mater.*, **18**, 1527 (2006).
- [10] A.P.Alivisatos, W.Gu, C.A.Larabell; *Annu.Rev.Biomed.Eng.*, **7**, 55 (2005).
- [11] B.A.Kairdolf, M.C.Mancini, A.M.Smith, S.M.Nie; *Anal.Chem.*, **80**, 3029 (2008).
- [12] J.L.West, N.Halas; *Annu.Rev.Biomed.Eng.*, **5**, 285 (2003).
- [13] D.Celik, M.Krueger, C.Veit, H.F.Schleiermacher, B.Zimmermann, S.Allard, I.Dumsch, U.Scherf, F.Rauscher, P.Niyamakom; *Solar Energy Materials and Solar Cells.*, **98**, 433 (2012).
- [14] V.Sholin, A.J.Breeze, I.E.Anderson, Y.Sahoo, D.Reddy, S.A.Carter; *Solar Energy Materials and Solar Cells.*, **92**, 1706 (2008).
- [15] C.B.Murray, D.J.Norris, M.G.Bawendi; *J.Am. Chem.Soc.*, **115**, 8706 (1993).
- [16] Z.A.Peng, X.G.Peng; *J.Am.Chem.Soc.*, **123**, 183 (2001).
- [17] X.G.Peng; *Chem.Eur.J.*, **8**, 335 (2002).
- [18] O.S.Oluwafemi, N.Revapasadu, A.J.Ramirez; *J.Cryst Growth*, **310**, 3230 (2008).
- [19] O.S.Oluwafemi; *Colloids Surf B Biointerfaces*, **73**, 382 (2009).
- [20] N.Gaponik, D.V.Talapin, A.L.Rogach, K.Hoppe, E.V.Shevchenko, A.Kornowski, A.Eychmuller, H.Weller; *J.Phys.Chem.B*, **106**, 7177 (2002).
- [21] A.L.Rogach, A.Kornowski, M.Y.Gao, A.Eychmuller, H.Weller; *J.Phys.Chem.*, **103**, 3065 (1999).
- [22] A.L.Rogach, D.Nagesha, J.W.Ostrander, M.Giersig, N.A.Kotov; *Chem.Mater.*, **12**, 2676 (2000).
- [23] Y.Wang, Z.Y.Tang, M.A.Correa-Duarte, I.Pastoriza-Santos, M.Giersig, N.A.Kotov, L.M.Liz-Marzan; *J.Phys.Chem.*, **108**, 15461 (2004).
- [24] I.Sondi, O.Siiman, E.Matijevic; *J.Colloid Interface Sci.*, **275**, 503 (2004).
- [25] W.W.Yu, E.Chang, R.Drezek, V.L.Colvin; *Biochem.Biophys.Res.Comm.*, **348**, 781 (2006).
- [26] X.H.Xue, J.Pan, H.M.Xie, J.H.Wang, S.Zhang; *Talanta*, **77**, 1808 (2009).
- [27] Z.B.Shang, Y.Wang, W.J.Jin; *Talanta*, **78**, 364 (2009).
- [28] B.Su, D.J.Fermin, J.P.Abid, N.Eugster, H.H.Girault; *J.Electroanal.Chem.*, **583**, 241 (2005).
- [29] Xingping Zhoua, Zhiyu Shaoa, Yoshio Kobayashic, Xiaqin Wangd, Noriaki Ohuchie; *Optical Materials*, **29**, 1048-1054 (2007).
- [30] L.Brus; *J.Phys.Chem.*, **90** (1986), 2555-2560 (2007).
- [31] H.Fu, L.W.Wang, A.Zunger; *Phys.Rev.B*, **59**, 5568-5574 (1999).
- [32] Singh, M.V.Limaye, S.K.Date, S.Gokhale, S.K.Kulkarni; *Phys.Rev.B*, **80**, 235421-235428 (2009).
- [33] S.L.Cumberland, K.M.Hanif, A.Javier, G.A.Khitrov, G.F.Strouse, S.M.Woessner, C.S.Yun; *Chem. Mater.*, **14**, 1576-1584 (2002).
- [34] J.N.Demas, G.A.Crosby; *J.Phys.Chem.*, **75**, 991-1024 (1971).
- [35] M.Y.Li, H.M.Zhou, H.Y.Zhang, P.Sun, K.Y.Yi, M.Wang, Z.Z.Dong, S.K.Xu; *J.Lumin.*, **130**, 1935-1940 (2010).
- [36] M.J.I.I.Bowers, J.R.McBride, S.J.Rosenthal; *J.Am. Chem.Soc.*, **127**, 15378-15379 (2005).
- [37] W.W.Yu, L.H.Qu, W.Z.Guo, X.G.Peng; *Chem. Mater.*, **15** (2003), 2854-2860 (2005).